

# Reactions of Rhodium Porphyrins with Lactones, Silanes, and Stannanes

Tadashi Mizutani,\* Tetsuya Uesaka, and Hisanobu Ogoshi\*

*Department of Synthetic Chemistry and Biological Chemistry, Faculty of Engineering,  
Kyoto University, Yoshida, Sakyo-ku, Kyoto 606-01, Japan*

Received June 3, 1994<sup>®</sup>

(2,3,7,8,12,13,17,18-Octaethylporphyrinato)rhodium(I) ( $\text{Rh}^{\text{I}}\text{OEP}$ ) cleaved the alkyl–oxygen bond of four-membered-ring and five-membered-ring lactones ( $\beta$ -propiolactone (**1**),  $\beta$ -butyrolactone (**2**), and  $\gamma$ -butyrolactone (**3**)) at room temperature to regioselectively yield ( $\omega$ -carboxyalkyl) $\text{Rh}^{\text{III}}\text{OEP}$ . [ $\{\text{Rh}^{\text{II}}\text{OEP}\}_2$ ] reacted with  $\text{R}^1_2\text{R}^2\text{MH}$  (**8**,  $\text{M} = \text{Si}$ ,  $\text{R}^1 = \text{R}^2 = \text{Et}$ ; **9**,  $\text{M} = \text{Si}$ ,  $\text{R}^1 = \text{R}^2 = \text{Ph}$ ; **10**,  $\text{M} = \text{Si}$ ,  $\text{R}^1 = \text{Me}$ ,  $\text{R}^2 = \text{Ph}$ ; **11**,  $\text{M} = \text{Si}$ ,  $\text{R}^1 = \text{Me}$ ,  $\text{R}^2 = \text{OEt}$ ; **16**,  $\text{M} = \text{Sn}$ ,  $\text{R}^1 = \text{R}^2 = \text{Bu}$ ; **17**,  $\text{M} = \text{Sn}$ ,  $\text{R}^1 = \text{R}^2 = \text{Ph}$ ) to yield  $\text{Rh}^{\text{III}}(\text{MR}^1_2\text{R}^2)\text{OEP}$ . These alkyl-, silyl-, and stannylrhodium complexes of OEP were characterized by  $^1\text{H}$ ,  $^{13}\text{C}$ ,  $^{29}\text{Si}$ , and  $^{119}\text{Sn}$  NMR, IR, UV-vis, and mass spectroscopy. (triethylsilyl) $\text{Rh}^{\text{III}}\text{OEP}$  crystallizes in the monoclinic space group  $C2/c$  with unit cell dimensions  $a = 17.14(8)$  Å,  $b = 14.94(5)$  Å,  $c = 31.22(5)$  Å, and  $\beta = 103.5(2)^\circ$ ; the density is  $1.28 \text{ g/cm}^3$  for  $Z = 8$ . The porphyrin plane is almost planar, and the rhodium metal resides on the plane. The  $\text{Rh}-\text{Si}$  distance is  $2.32(1)$  Å, and all the eight ethyl groups on the pyrroles are directed toward the triethylsilyl group. The present method has proved to be a facile way to prepare bimetallic rhodium complexes of porphyrin.

Rhodium–porphyrin complexes are of interest for their diverse reactivities depending on the oxidation state of the rhodium metal.<sup>1,2</sup> Similar reactions were found to take place with both Rh porphyrin and Co porphyrin. The Rh porphyrin has been studied as a model of the vitamin  $\text{B}_{12}$  coenzyme.<sup>3</sup> Rh(I) porphyrin, for example, is nucleophilic and undergoes numerous nucleophilic substitution and addition reactions such as conjugated addition to the  $\alpha,\beta$ -unsaturated carbonyl compounds<sup>2</sup> and cleavage of three- or four-membered cyclic ethers.<sup>4</sup> A Rh(II) porphyrin dimer undergoes radical reactions with olefins and acetylenes.<sup>5</sup> Wayland et al.<sup>6</sup> reported that (tetramesitylporphyrinato)rhodium(II) can cleave a C–H bond of methane. A Rh(III) porphyrin is electrophilic. It reacts with organolithium compounds<sup>2</sup> and acts as a Lewis acid catalyst.<sup>7</sup> These reactions, especially those forming a Rh–C bond, are useful for prediction of possible elementary reactions taking place in Co–C species derived from vitamin  $\text{B}_{12}$ , since the similarity between the reactivity of the Rh(II) porphyrin and the Co(II) porphyrin has been noticed.<sup>8</sup> Recently, insertion reactions of carbenes catalyzed by rhodium(III) porphyrins have attracted much

interest.<sup>9</sup> In this paper we report that a nucleophilic Rh(I) porphyrin reacts with a four- or five-membered ring lactone at the alkoxide carbon to give ( $\omega$ -carboxyalkyl) $\text{Rh}^{\text{III}}\text{OEP}$ . Also, the  $\text{Rh}^{\text{II}}\text{OEP}$  dimer reacts with hydrosilane or hydrostannane to give (trialkylsilyl) $\text{Rh}^{\text{III}}\text{OEP}$  or (trialkylstannyl) $\text{Rh}^{\text{III}}\text{OEP}$ , respectively.

## Results and Discussion

**Reaction of Rhodium(I) Octaethylporphyrin with Lactones.** Reactions of  $\text{Rh}^{\text{I}}\text{OEP}$  with four-, five-, and six-membered ring lactones and ethyl acetate (as a representative of a linear ester) were performed at room temperature under Ar (Scheme 1). Products and yields of the reactions are summarized in Table 1. Four- and five-membered-ring lactones gave alkyl–rhodium complexes, while the six-membered-ring lactone and ethyl acetate did not. Therefore, the ring size of the lactone is one of the important factors in the limitation of this reaction. The strain energies are 8.8 kcal/mol for **3** and 11.2 kcal/mol for **4** (calorimetry),<sup>10a</sup> 7.3 kcal/mol for **3** and 10.0 kcal/mol for **4** (ab initio, HF/6-31G\*),<sup>10a</sup> and 8.70 kcal/mol for **3** and 10.36 kcal/mol for **4** (MM3).<sup>10b</sup> These data indicate that the six-membered-ring lactone (**4**) is more strained than the five-membered-ring lactone (**3**) by 1.7–2.7 kcal/mol. The difference in strain energy alone, therefore, cannot account for the difference in reactivity.

The second important result is the regiospecificity of the reaction. In the reaction, the alkyl–oxygen bond of lactone is cleaved in preference to the acyl–oxygen

\* Abstract published in *Advance ACS Abstracts*, November 1, 1994.  
(1) Guillard, R.; Kadish, K. M. *Chem. Rev.* 1988, 88, 1121.  
(2) Ogoshi, H.; Setsune, J.; Omura, T.; Yoshida, Z. *J. Am. Chem. Soc.* 1975, 97, 6461.

(3) For examples of reactions of Co–porphyrins, see: (a) Ogoshi, H.; Kikuchi, Y.; Yamaguchi, T.; Toi, H.; Aoyama, Y. *Organometallics* 1987, 6, 2175. (b) Setsune, J.-i.; Ishimaru, Y.; Moriyama, T.; Kitao, T. *J. Chem. Soc., Chem. Commun.* 1991, 555. (c) Gridnev, A. A.; Ittel, S. D.; Fryd, M.; Wayland, B. B. *J. Am. Chem. Soc., Chem. Commun.* 1993, 1010. (d) Gridnev, A. A.; Ittel, S. D.; Fryd, M.; Wayland, B. B. *Organometallics* 1993, 12, 4871.

(4) Ogoshi, H.; Setsune, J.; Yoshida, Z. *J. Organomet. Chem.* 1980, 185, 95.

(5) (a) Ogoshi, H.; Setsune, J.; Yoshida, Z. *J. Am. Chem. Soc.* 1977, 99, 3869. (b) Paonessa, R. S.; Thomas, N. C.; Halpern, J. *J. Am. Chem. Soc.* 1985, 107, 4333.

(6) Sherry, A. E.; Wayland, B. B. *J. Am. Chem. Soc.* 1990, 112, 1259.

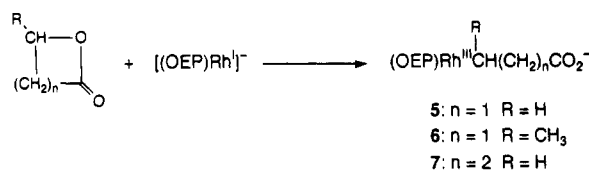
(7) Aoyama, Y.; Yamagishi, A.; Tanaka, Y.; Toi, H.; Ogoshi, H. *J. Am. Chem. Soc.* 1987, 109, 4735.

(8) Brown, K. L. In *B<sub>12</sub>*; Dolphin, D., Ed.; Wiley: New York, 1982; Vol. I, p 245.

(9) (a) Callot, H. J.; Metz, F.; Piechocki, C. *Tetrahedron* 1982, 38, 2365. (b) Maxwell, J. L.; Brown, K. C.; Bartley, D. W.; Kodadek, T. *Science* 1992, 256, 1544.

(10) (a) Wiberg, K. B.; Waldron, R. F. *J. Am. Chem. Soc.* 1991, 113, 7697. (b) Allinger, N. L.; Zhu, Z. S.; Chen, K. *J. Am. Chem. Soc.* 1992, 114, 6120.

Scheme 1

Table 1. Reactions of Rh<sup>I</sup>OEP with Lactones

Substrate	Product	Yield (%)
1	(OEP)Rh <sup>III</sup> CH <sub>2</sub> CH <sub>2</sub> CO <sub>2</sub> H	72
2	(OEP)Rh <sup>III</sup> CH(CH <sub>3</sub> )CH <sub>2</sub> CO <sub>2</sub> H	68
3	(OEP)Rh <sup>III</sup> CH <sub>2</sub> CH <sub>2</sub> CH <sub>2</sub> CO <sub>2</sub> H	45
4	No reaction	
AcOE <sup>t</sup>	No reaction	

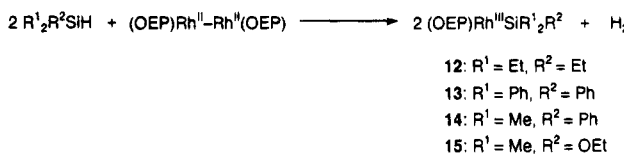
bond. Spectroscopic data of the product obtained from Rh<sup>I</sup>OEP and  $\beta$ -butyrolactone showed that the Rh atom is not bonded to the carbonyl carbon (C1) but bonded to the alkoxide carbon (C3). The <sup>1</sup>H NMR signal at  $\delta$  -6.42 ppm exhibits a coupling constant of  $J$  = 2.8 Hz besides the vicinal H–H coupling, which can be ascribed to the coupling between <sup>1</sup>H and <sup>103</sup>Rh. If the rhodium were bonded to the carbonyl carbon, the expected chemical shift of the signal in the highest magnetic field would be close to -3.77 ppm, which is the chemical shift of the proton  $\beta$  to the Rh atom of [Rh<sup>III</sup>{CO(CH<sub>2</sub>)<sub>4</sub>CH<sub>3</sub>}<sub>2</sub>OEP] in CDCl<sub>3</sub>.<sup>11</sup> Therefore, the signal appearing at -6.47 ppm is assignable to the proton  $\alpha$  to the Rh atom. The <sup>13</sup>C NMR signal at  $\delta$  6.76 ppm recorded with complete <sup>1</sup>H decoupling exhibits a coupling constant of  $J$  = 27.9 Hz, which can be ascribed to the coupling between <sup>13</sup>C and <sup>103</sup>Rh. The <sup>1</sup>H–<sup>13</sup>C HSQC spectrum indicated that the two signals noted above (<sup>1</sup>H and <sup>13</sup>C) are correlated and that the hydrogen and the carbon noted above are directly bonded to each other. The IR spectrum showed a peak at 1706 cm<sup>-1</sup>, which is ascribed to the C=O stretching of the carboxyl group. All these data are consistent with structure 5. It is noteworthy that the reaction is readily completed at room temperature. This can be ascribed to the high nucleophilicity of the Rh(I) porphyrin. The observed regioselectivity is similar to that observed for thiol,<sup>12</sup> selenium,<sup>13</sup> silicon,<sup>14</sup> and other<sup>15</sup> nucleophiles in their reactions with

(11) Ogoshi, H.; Setsune, J.; Nanbo, Y.; Yoshida, Z. *J. Organomet. Chem.* 1978, 159, 329.

(12) Plieninger, H. *Chem. Ber.* 1950, 83, 265.

(13) (a) Miyoshi, N.; Ishii, H.; Murai, S.; Sonoda, N. *Chem. Lett.* 1979, 873. (b) Scarborough, R. M., Jr.; Toder, B. H.; Smith, A. B., III. *J. Am. Chem. Soc.* 1980, 102, 3904. (c) Liotta, D.; Sunay, U.; Santiesteban, H.; Markiewicz, W. *J. Org. Chem.* 1981, 46, 2605.

Scheme 2

Table 2. Reactions of [Rh<sup>II</sup>OEP]<sub>2</sub> with Silanes

substrate	product	yield (%)	<sup>29</sup> Si NMR	
			$\delta$ (ppm)	$J_{\text{Si}-\text{Rh}}$ (Hz)
Et <sub>3</sub> SiH (8)	Rh <sup>III</sup> (SiEt <sub>3</sub> )OEP (12)	54	51.98	29.3
Ph <sub>3</sub> SiH (9)	Rh <sup>III</sup> (SiPh <sub>3</sub> )OEP (13)	65	11.56	35.7
Me <sub>2</sub> PhSiH (10)	Rh <sup>III</sup> (SiPhMe <sub>2</sub> )OEP (14)	44	28.30	30.2
(EtO) <sub>2</sub> Me <sub>2</sub> SiH (11)	Rh <sup>III</sup> (SiMe <sub>2</sub> (OEt))OEP (15)	42	37.24	30.5

lactones.<sup>16</sup> In these reactions, a tendency is observed that "soft" nucleophiles attack the alkyl carbon to give alkyl–oxygen cleavage.<sup>13c,15b</sup> On the basis of these results, we suggest that the rhodium(I) porphyrin is a soft nucleophile.

**Reaction of Rhodium(I) Octaethylporphyrin with Lactams.** Reactions of [Rh<sup>I</sup>OEP] with lactams ( $\beta$ -propiolactam,  $\gamma$ -butyrolactam,  $\delta$ -valerolactam, and 1-methyl-2-pyrrolidinone) were also investigated. In contrast to lactones, no formation of alkyl–rhodium complexes was detected using <sup>1</sup>H NMR. The nucleophilic ring opening reaction is thus sensitive to the differences in leaving group structures ( $-\text{CO}_2^-$  vs  $-\text{CONH}^-$ ).

**Reaction of Rh<sup>II</sup>OEP Dimer with Organosilanes.** The reaction of Rh complexes with organosilanes is interesting because some Rh complexes constitute an important group of the hydrosilylation catalyst. The development of versatile preparative methods of transition-metal–silicon complexes is thus desired. By using the metalloradical reactivity<sup>17</sup> of the Rh<sup>II</sup>OEP dimer, the preparation of silylrhodium complexes was explored.<sup>18</sup> Hydrosilanes reacted with the Rh<sup>II</sup>OEP dimer smoothly to give silylrhodium complexes of OEP (Scheme 2). The products, yields, and <sup>29</sup>Si NMR data (chemical shifts  $\delta$  and coupling constants  $J_{\text{Si}-\text{Rh}}$ ) are listed in Table 2. The <sup>29</sup>Si NMR chemical shifts of the starting silanes were 0.15 ppm (8), -17.75 ppm (9), and -17.50 ppm (10).<sup>13</sup> Therefore, the <sup>29</sup>Si chemical shift displacements upon rhodium–silicon bond formation ranged from 30 to 50 ppm, which is characteristic of the chemical shift displacement of <sup>29</sup>Si bonded to a transition metal.<sup>19</sup> These NMR data indicate that triethylsilane (8), triphenylsilane (9), dimethylphenylsilane (10), and dimethylethoxysilane reacted with [Rh<sup>II</sup>OEP]<sub>2</sub> to form (trialkylsilyl)rhodium complexes.<sup>20</sup> Because the yields of 8 and 9 exceed 50% on the basis of [Rh<sup>II</sup>OEP]<sub>2</sub>, both Rh

(14) Kolb, M.; Barth, J. *Synth. Commun.* 1981, 11, 763.

(15) (a) Ali, S. M.; Chapleo, C. B.; Finch, M. A. W.; Roberts, S. M.; Woolley, G. T.; Cave, R. J.; Newton, R. F. *J. Chem. Soc., Perkin Trans. I* 1980, 2093. (b) Arnold, L. D.; Kalantar, T. H.; Vederas, J. C. *J. Am. Chem. Soc.* 1985, 107, 7105.

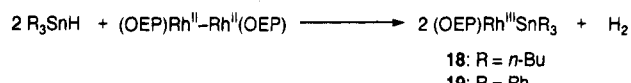
(16) For a review on ester cleavage via S<sub>N</sub>2-type dealkylation, see: McMurry, J. *Org. React.* 1976, 24, 187.

(17) Paonessa, R. S.; Thomas, N. C.; Halpern, J. *J. Am. Chem. Soc.* 1985, 107, 4333.

(18) For examples of the reaction of silanes and transition metal complexes, see: (a) Baay, Y. L.; MacDiarmid, A. G. *Inorg. Chem.* 1969, 8, 986. (b) Sissak, A.; Ungvary, F.; Marko, L. *Organometallics* 1986, 5, 1019.

(19) Marsmann, H. In *<sup>29</sup>Si-NMR Spectroscopic Results*; Diehl, P., Fluck, E., Kosfeld, R., Eds.; Springer-Verlag: Berlin, 1981; pp 66–235.

Scheme 3

Table 3. Reactions of  $[(\text{OEP})\text{Rh}^{\text{II}}]_2$  with Stannanes

substrate	product	yield (%)	$^{119}\text{Sn}$ NMR	
			$\delta$ (ppm)	$J_{^{119}\text{Sn}-^{103}\text{Rh}}$ (Hz)
n-Bu <sub>3</sub> SnH (16)	Rh <sup>II</sup> (SnBu <sub>3</sub> )OEP (18)	49	118.3	314.2
Ph <sub>3</sub> SnH (17)	Rh <sup>II</sup> (SnPh <sub>3</sub> )OEP (19)	44	-121.6	412.9

Table 4. Crystal Data for  $(\text{OEP})\text{RhSiEt}_3$  (12)

formula	C <sub>42</sub> H <sub>59</sub> N <sub>4</sub> SiRh
fw	750.95
space group	C <sub>2</sub> /c
a, Å	17.14(8)
b, Å	14.94(5)
c, Å	31.22(5)
$\beta$ , deg	103.5(2)
V, Å <sup>3</sup>	7774(43)
Z	8
$\rho$ (calcd), g/cm <sup>3</sup>	1.28
temp, °C	-120
cryst dimens, mm	0.25 × 0.25 × 0.25
radiation	graphite-monochromated Mo K $\alpha$ radiation, 12 kW rotating anode generator
linear abs coeff, cm <sup>-1</sup>	5.0
detector aperture, mm	9.0 (horiz), 13.0 (vert)
scan type	$\omega-2\theta$
scan rate, deg/min	16.0 (in $\omega$ )
2 $\theta$ limits, deg	0.0 < 2 $\theta$ < 60.4
no. of rflns measd	12 149 total, 11 779 unique
no. of rflns used	9548
no. of variables	601
R	0.063
R <sub>w</sub>	0.078

atoms of  $[\text{Rh}^{\text{II}}\text{OEP}]_2$  are incorporated in the rhodium-silyl complexes.

Similarly, hydrostannanes react with the Rh(II) dimer to afford stannyly-rhodium complexes of OEP (Scheme 3). The products and  $^{119}\text{Sn}$  NMR data are listed in Table 3. Coupling constants of 300–400 Hz were observed in the  $^{119}\text{Sn}$  NMR spectra of the stannyly-rhodium complexes, supporting the notion that a direct bond between Rh and Sn exists in the product.<sup>21,22</sup>

$\text{Rh}^{\text{III}}(\text{SiEt}_3)\text{OEP}$  crystallizes in the monoclinic space group C<sub>2</sub>/c with eight porphyrin molecules per unit cell. Crystal data, positional parameters, and intramolecular distances and angles are listed in Tables 4–7. The porphyrin is almost planar, and the rhodium atom resides on the plane (Figure 1). The displacement of the Rh atom from the least-squares plane of four nitrogen atoms was 0.090 Å, which is comparable to those of similar rhodium porphyrins ((OEP)RhMe, 0.051 Å;<sup>23</sup> (OEP)RhCHO, 0.080 Å;<sup>24</sup> (OEP)RhH, 0.010 Å;<sup>24</sup>

(20) For an example of a compound having a Rh-Si bond, see: Bennett, M. A.; Patmore, D. J. *Inorg. Chem.* 1971, 10, 2387.

(21) Coupling constants  $J_{^{103}\text{Rh}-^{119}\text{Sn}}$  of 102–615 Hz were reported for stannyly-rhodium complexes; see: (a) Ruiz, J.; Spencer, C. M.; Mann, B. E.; Taylor, B. F.; Maitlis, P. M. *J. Organomet. Chem.* 1987, 325, 253. (b) Fridaldo, L.; Garralda, M. A.; Hernandez, R.; Ibarlucea, L. *Inorg. Chim. Acta* 1993, 207, 121. (c) Calton, L.; Weber, R. *Inorg. Chem.* 1993, 32, 4169.

(22) The phenyl group on stannanes causes upfield shifts of the  $^{119}\text{Sn}$  chemical shifts. For example, chemical shifts of  $^{119}\text{Sn}$  are -164.5 (Ph<sub>3</sub>SnH), -91.4 (Bu<sup>n</sup><sub>3</sub>SnH), -85.5 ((Ph<sub>3</sub>Sn)<sub>2</sub>O), and 82.0 ((Bu<sup>n</sup><sub>3</sub>Sn)<sub>2</sub>O), see: Wrackmeyer, B. In *Annual Reports on NMR Spectroscopy*; Webb, G. A. Ed.; Academic Press: London, 1985; Vol. 16, p 73.

(23) Takenaka, A.; Syal, S. K.; Sasada, Y.; Omura, T.; Ogoshi, H.; Yoshida, Z. *Acta Crystallogr., Sect. B: Struct. Crystallogr. Cryst. Chem.* 1976, B32, 62.

(24) Jones, N. L.; Carroll, P. J.; Wayland, B. B. *Organometallics* 1986, 5, 33.

Table 5. Positional Parameters for Non-Hydrogen Atoms of 12

atom	x	y	z	B(eq), Å <sup>2</sup>
Rh(1)	0.09209(2)	-0.00455(2)	0.341049(9)	1.73(1)
Si(1)	0.04240(7)	-0.00308(7)	0.40394(4)	2.35(2)
N(1)	-0.0185(2)	0.0151(2)	0.3010(1)	1.8(1)
N(2)	0.1107(2)	0.1296(2)	0.3449(1)	1.9(1)
N(3)	0.2068(2)	-0.0248(2)	0.3760(1)	2.1(1)
N(4)	0.0775(2)	-0.1388(2)	0.3326(1)	2.0(1)
C(1)	-0.0726(2)	-0.0491(2)	0.2822(1)	1.9(1)
C(2)	-0.1452(2)	-0.0071(2)	0.2566(1)	2.1(1)
C(3)	-0.1332(2)	0.0827(2)	0.2605(1)	2.1(1)
C(4)	-0.0541(2)	0.0963(2)	0.2885(1)	1.9(1)
C(5)	-0.0193(2)	0.1787(2)	0.3002(1)	2.2(1)
C(6)	0.0573(2)	0.1948(2)	0.3263(1)	2.2(1)
C(7)	0.0930(2)	0.2826(2)	0.3368(1)	2.5(1)
C(8)	0.1684(2)	0.2690(3)	0.3616(1)	2.4(1)
C(9)	0.1793(2)	0.1738(3)	0.3665(1)	2.2(1)
C(10)	0.2488(2)	0.1319(3)	0.3887(1)	2.4(1)
C(11)	0.2618(2)	0.0399(3)	0.3936(1)	2.3(1)
C(12)	0.3362(2)	-0.0015(3)	0.4177(1)	2.6(1)
C(13)	0.3246(2)	-0.0920(3)	0.4140(1)	2.8(1)
C(14)	0.2440(2)	-0.1053(3)	0.3877(1)	2.3(1)
C(15)	0.2088(2)	-0.1882(3)	0.3753(1)	2.4(1)
C(16)	0.1322(2)	-0.2040(2)	0.3504(1)	2.1(1)
C(17)	0.0977(2)	-0.2918(2)	0.3389(1)	2.2(1)
C(18)	0.0221(2)	-0.2783(2)	0.3136(1)	2.1(1)
C(19)	0.0099(2)	-0.1828(2)	0.3098(1)	2.0(1)
C(20)	-0.0592(2)	-0.1407(2)	0.2863(1)	2.0(1)
C(21)	-0.2192(2)	-0.0557(3)	0.2325(1)	2.5(1)
C(22)	-0.2755(3)	-0.0810(4)	0.2617(2)	4.1(2)
C(23)	-0.1906(2)	0.1564(3)	0.2427(1)	2.5(1)
C(24)	-0.2373(3)	0.1879(4)	0.2748(2)	3.7(2)
C(25)	0.0496(3)	0.3691(3)	0.3228(2)	3.4(2)
C(26)	-0.0063(4)	0.3951(4)	0.3519(3)	5.1(3)
C(27)	0.2291(3)	0.3372(3)	0.3833(2)	3.2(2)
C(28)	0.2330(4)	0.3485(4)	0.4317(2)	4.6(2)
C(29)	0.4073(3)	0.0492(3)	0.4437(2)	3.2(2)
C(30)	0.3948(4)	0.0810(5)	0.4874(2)	4.8(3)
C(31)	0.3802(3)	-0.1654(3)	0.4343(2)	3.7(2)
C(32)	0.3634(6)	-0.2000(6)	0.4764(3)	6.2(4)
C(33)	0.1384(3)	-0.3780(3)	0.3555(2)	2.8(2)
C(34)	0.1325(4)	-0.4005(4)	0.4019(2)	4.4(2)
C(35)	-0.0410(3)	-0.3475(3)	0.2957(1)	2.5(1)
C(36)	-0.0986(3)	-0.3621(4)	0.3248(2)	3.7(2)
C(37)	-0.066(1)	0.0480(9)	0.3906(4)	13.3(8)
C(38)	-0.1074(8)	0.044(1)	0.4265(7)	16(1)
C(39)	0.0989(6)	0.083(1)	0.4481(2)	31(1)
C(41)	0.040(1)	-0.1138(6)	0.4283(5)	15.9(8)
C(42)	-0.0221(8)	-0.165(1)	0.4298(8)	27(2)

(OEP)RhCONH(xylyl), 0.072 Å<sup>25</sup>). The Rh-Si distance was 2.32(1) Å. All the ethyl groups on the porphyrin periphery are directed toward the triethylsilyl group. The crystal packing indicates that the aromatic part of the molecule is in contact with the aromatic part of the next molecule and the aliphatic part is in contact with the aliphatic part of the next molecule (Figure 2). This intermolecular interaction mode accounts for the fact that all the ethyl groups are pointed in the same direction.

Both the silyl and the stannyly complexes of the rhodium porphyrin are relatively stable. These results indicate that the present method provides a facile way to prepare bimetallic rhodium complexes of porphyrin.

## Experimental Section

**General Procedures.**  $^1\text{H}$  and  $^{13}\text{C}$  NMR spectra were obtained using a JEOL A-500 spectrometer, a JEOL GX-400 spectrometer, or a JEOL JNM FX 90Q FT NMR spectrometer, and chemical shifts are reported relative to internal Me<sub>4</sub>Si.

(25) Poszmk, G.; Carroll, P. J.; Wayland, B. B. *Organometallics* 1993, 12, 3410.

**Table 6. Intramolecular Distances Involving the Non-Hydrogen Atoms of 12<sup>a</sup>**

Rh(1)–Si(1)	2.32(1)	C(7)–C(25)	1.50(6)
Rh(1)–N(1)	2.03(3)	C(8)–C(9)	1.44(5)
Rh(1)–N(2)	2.03(3)	C(8)–C(27)	1.50(6)
Rh(1)–N(3)	2.04(3)	C(9)–C(10)	1.38(5)
Rh(1)–N(4)	2.03(3)	C(10)–C(11)	1.40(6)
Si(1)–C(37)	2.0(1)	C(11)–C(12)	1.46(5)
Si(1)–C(39)	2.0(1)	C(12)–C(13)	1.37(6)
Si(1)–C(41)	1.82(7)	C(12)–C(29)	1.50(6)
N(1)–C(1)	1.37(4)	C(13)–C(14)	1.45(5)
N(1)–C(4)	1.37(4)	C(13)–C(31)	1.49(6)
N(2)–C(6)	1.37(5)	C(14)–C(15)	1.39(5)
N(2)–C(9)	1.38(5)	C(15)–C(16)	1.38(5)
N(3)–C(11)	1.37(5)	C(16)–C(17)	1.45(5)
N(4)–C(16)	1.37(5)	C(17)–C(33)	1.50(5)
N(4)–C(19)	1.38(5)	C(18)–C(19)	1.44(5)
C(1)–C(20)	1.39(5)	C(19)–C(20)	1.39(5)
C(2)–C(3)	1.36(5)	C(21)–C(22)	1.52(7)
C(2)–C(21)	1.50(5)	C(23)–C(24)	1.50(7)
C(3)–C(4)	1.44(5)	C(25)–C(26)	1.52(8)
C(3)–C(23)	1.49(5)	C(27)–C(28)	1.50(7)
C(4)–C(5)	1.38(5)	C(29)–C(30)	1.51(8)
C(5)–C(6)	1.39(5)	C(31)–C(32)	1.5(1)
C(6)–C(7)	1.45(5)	C(33)–C(34)	1.51(8)
C(7)–C(8)	1.36(5)	C(35)–C(36)	1.50(7)
C(37)–C(38)	1.5(2)		
C(41)–C(42)	1.3(2)		

<sup>a</sup> Distances are in angstroms. Estimated standard deviations in the least significant figure are given in parentheses.

<sup>29</sup>Si NMR spectra were recorded on a JEOL A-500 spectrometer operating at 100 MHz with NOE-eliminated complete <sup>1</sup>H decoupling. Chemical shifts are reported relative to internal Me<sub>4</sub>Si. UV-vis spectra were recorded on either a Hitachi U-3410 spectrometer or a Hewlett-Packard 8452 diode array spectrophotometer with a thermostated cell compartment. Mass spectra were obtained with a JEOL JMS DX-300 mass spectrometer. High-resolution mass spectra were recorded on a JEOL JMS SX-102A instrument. Thin-layer chromatography (TLC) was performed on either Merck Kieselgel 60 F<sub>254</sub> or DC-Alufolien aluminium oxide 60 F<sub>254</sub> neutral (type E). Single-crystal X-ray diffraction was performed on a Rigaku AFC7R diffractometer.

**Materials.** Octaethylporphyrin (OEP) was prepared according to the published method.<sup>26</sup> [Rh<sup>III</sup>I(OEP)] was prepared by treating OEP with Rh<sub>2</sub>(CO)<sub>8</sub>, followed by oxidation with I<sub>2</sub>. [Rh<sup>II</sup>OEP]<sub>2</sub> was prepared according to the published method.<sup>27</sup>

[Rh<sup>III</sup>(CH<sub>2</sub>CH<sub>2</sub>CO<sub>2</sub>H)OEP] (5). [Rh<sup>III</sup>I(OEP)] (11.4 mg, 14.9 μmol) was dissolved in dry and degassed ethanol at 50 °C, and NaBH<sub>4</sub> (2.6 mg, 68.7 μmol) in 0.5 M aqueous NaOH (2 mL) was added under Ar. The solution turned from red to deep orange. After it was stirred at 50 °C for 1 h under Ar, the solution was cooled to room temperature, and β-propiolactone (1; 0.1 mL, 1.59 mmol) was added. The color changed immediately to orange. After the solution was stirred for 30 min, the ethanol was evaporated under reduced pressure. The residue was washed with water and dried. The product was recrystallized from THF–MeOH; yield 6.8 mg (72%). <sup>1</sup>H NMR (Me<sub>2</sub>SO-*d*<sub>6</sub>, 500 MHz): δ 10.05 (s, 4H, meso), 4.08 (q, *J* = 14 Hz, *J* = 7.8 Hz, 8H, CH<sub>2</sub>CH<sub>3</sub>), 4.03 (q, *J* = 14 Hz, *J* = 7.8 Hz, 8H, CH<sub>2</sub>CH<sub>3</sub>), 1.85 (t, *J* = 7.8 Hz, 24H, CH<sub>2</sub>CH<sub>3</sub>), –4.60 (t, *J* = 8.7 Hz, 2H, RhCH<sub>2</sub>CH<sub>2</sub>CO<sub>2</sub>H), –6.42 (td, *J* = 8.7 Hz, *J*<sub>H–Rh</sub> = 2.8 Hz, 2H, RhCH<sub>2</sub>CH<sub>2</sub>CO<sub>2</sub>H), IR (KBr): 3400–2500, 2964, 2981, 2869, 1703, 1274, 1021 cm<sup>-1</sup>. UV-vis (CHCl<sub>3</sub>): λ<sub>max</sub> (log ε) 386.4 (0.77), 392.8 (0.80), 509.9 (0.084), 542.9 (0.27). FAB MS (*m*-nitrobenzyl alcohol matrix): *m/z* 708 (M<sup>+</sup>, 100). HRMS: calcd for C<sub>40</sub>H<sub>51</sub>N<sub>4</sub>O<sub>2</sub>Rh 708.291, found 708.297.

[Rh<sup>III</sup>(CH<sub>2</sub>CH<sub>2</sub>CH<sub>2</sub>CO<sub>2</sub>H)OEP] (7). Yield: 45%. <sup>1</sup>H NMR (Me<sub>2</sub>SO-*d*<sub>6</sub>, 500 MHz): δ 10.01 (s, 4H, meso), 4.06 (q, *J* = 14 Hz, *J* = 7.7 Hz, 8H, CH<sub>2</sub>CH<sub>3</sub>), 4.00 (q, *J* = 14 Hz, *J* = 7.7 Hz,

**Table 7. Intramolecular Bond Angles Involving the Non-Hydrogen Atoms of 12<sup>a</sup>**

Si(1)–Rh(1)–N(1)	92.6(9)	Rh(1)–N(4)–C(19)	127(2)
Si(1)–Rh(1)–N(2)	91.4(9)	C(16)–N(4)–C(19)	106(3)
Si(1)–Rh(1)–N(3)	93(1)	N(1)–C(1)–C(2)	110(3)
Si(1)–Rh(1)–N(4)	93.5(9)	N(1)–C(1)–C(20)	125(3)
N(1)–Rh(1)–N(2)	90(1)	C(2)–C(1)–C(20)	125(3)
N(1)–Rh(1)–N(3)	175(1)	C(1)–C(2)–C(3)	107(3)
N(1)–Rh(1)–N(4)	90(1)	C(1)–C(2)–C(21)	125(3)
N(2)–Rh(1)–N(3)	90(1)	C(3)–C(2)–C(21)	128(3)
N(2)–Rh(1)–N(4)	175(1)	C(2)–C(3)–C(4)	107(3)
N(3)–Rh(1)–N(4)	90(1)	C(2)–C(3)–C(23)	128(4)
Rh(1)–Si(1)–C(37)	110(2)	C(4)–C(3)–C(23)	124(3)
Rh(1)–Si(1)–C(39)	113(2)	N(1)–C(4)–C(3)	110(3)
Rh(1)–Si(1)–C(41)	113(3)	N(1)–C(4)–C(5)	125(3)
C(37)–Si(1)–C(39)	100(7)	C(3)–C(4)–C(5)	125(3)
C(37)–Si(1)–C(41)	109(6)	C(4)–C(5)–C(6)	127(4)
C(39)–Si(1)–C(41)	111(7)	N(2)–C(6)–C(5)	125(3)
Rh(1)–N(1)–C(1)	127(2)	N(2)–C(6)–C(7)	110(3)
Rh(1)–N(1)–C(4)	126(2)	C(5)–C(6)–C(7)	125(4)
C(1)–N(1)–C(4)	107(3)	C(6)–C(7)–C(8)	107(3)
Rh(1)–N(2)–C(6)	127(3)	C(6)–C(7)–C(25)	124(4)
Rh(1)–N(2)–C(9)	127(3)	C(8)–C(7)–C(25)	129(4)
C(6)–N(2)–C(9)	106(3)	C(7)–C(8)–C(9)	107(3)
Rh(1)–N(3)–C(11)	127(3)	C(7)–C(8)–C(27)	129(4)
Rh(1)–N(3)–C(14)	127(3)	C(9)–C(8)–C(27)	124(4)
C(11)–N(3)–C(14)	106(3)	Rh(1)–N(4)–C(16)	127(2)
N(2)–C(9)–C(8)	110(3)	C(18)–C(17)–C(33)	129(4)
N(2)–C(9)–C(10)	124(4)	C(17)–C(18)–C(19)	107(3)
C(8)–C(9)–C(10)	125(4)	C(17)–C(18)–C(35)	128(4)
C(9)–C(10)–C(11)	127(4)	C(19)–C(18)–C(35)	125(3)
N(4)–C(19)–C(18)	110(3)	C(18)–C(19)–C(20)	125(3)
N(4)–C(19)–C(20)	125(3)	C(1)–C(20)–C(19)	127(3)
N(3)–C(11)–C(10)	125(4)	C(2)–C(21)–C(22)	114(4)
N(3)–C(11)–C(12)	110(3)	C(3)–C(23)–C(24)	113(4)
C(10)–C(11)–C(12)	125(4)	C(12)–C(29)–C(30)	112(4)
C(11)–C(12)–C(13)	106(3)	C(13)–C(31)–C(32)	113(5)
C(11)–C(12)–C(29)	124(4)	Si(1)–C(37)–C(38)	115(10)
C(13)–C(12)–C(29)	129(4)	C(17)–C(33)–C(34)	113(4)
C(12)–C(13)–C(14)	107(4)	C(18)–C(35)–C(36)	113(4)
C(12)–C(13)–C(31)	129(4)	Si(1)–C(41)–C(42)	129(12)
C(14)–C(13)–C(31)	125(4)	C(16)–C(17)–C(33)	124(4)
N(3)–C(14)–C(13)	111(3)	C(7)–C(25)–C(26)	113(4)
N(3)–C(14)–C(15)	124(3)	C(8)–C(27)–C(28)	113(4)
C(13)–C(14)–C(15)	125(4)	N(4)–C(16)–C(17)	110(3)
C(14)–C(15)–C(16)	127(4)	C(15)–C(16)–C(17)	125(3)
N(4)–C(16)–C(15)	125(4)	C(16)–C(17)–C(18)	107(3)

<sup>a</sup> Angles are in degrees. Estimated standard deviations in the least significant figure are given in parentheses.

8H, CH<sub>2</sub>CH<sub>3</sub>), 1.83 (t, *J* = 7.7 Hz, 24H, CH<sub>2</sub>CH<sub>3</sub>), –1.22 (t, *J* = 8.0 Hz, 2H, RhCH<sub>2</sub>CH<sub>2</sub>CH<sub>2</sub>CO<sub>2</sub>H), –4.93 (quintet, *J* = 7.8 Hz, 2H, RhCH<sub>2</sub>CH<sub>2</sub>CH<sub>2</sub>CO<sub>2</sub>H), –6.47 (td, *J* = 8.0 Hz, *J*<sub>H–Rh</sub> = 1.8 Hz, 2H, RhCH<sub>2</sub>CH<sub>2</sub>CH<sub>2</sub>CO<sub>2</sub>H). <sup>13</sup>C NMR (125 MHz, THF-*d*<sub>8</sub>): δ 172.16 (s, COOH), 142.21 (s, pyrrole α), 141.23 (s, pyrrole β), 99.09 (s, meso), 31.81 (s, α-C to carboxy), 22.10 (s, β-C to carboxy), 20.42 (s, CH<sub>2</sub>CH<sub>3</sub>), 18.95 (s, CH<sub>2</sub>CH<sub>3</sub>), 6.76 (d, *J*<sub>C–Rh</sub> = 27.9 Hz, γ-C to carboxy). IR (KBr): 3300–2500, 2962, 2929, 2868, 1706, 1274, 1019 cm<sup>-1</sup>. UV-vis (CHCl<sub>3</sub>): λ<sub>max</sub> (log ε) 385.8 (1.067), 391.8 (1.12), 509.6 (0.12), 542.6 (0.39). FAB MS (*m*-nitrobenzyl alcohol matrix): *m/z* 722 (M<sup>+</sup>, 100). HRMS: calcd for C<sub>40</sub>H<sub>51</sub>N<sub>4</sub>O<sub>2</sub>Rh 722.307, found 722.306.

[Rh<sup>III</sup>{CH(CH<sub>3</sub>)CH<sub>2</sub>CO<sub>2</sub>H}OEP] (6). Yield: 68%. <sup>1</sup>H NMR (CDCl<sub>3</sub>, 500 MHz): δ 10.05 (s, 4H, meso), 3.92–4.18 (m, 16H, CH<sub>2</sub>CH<sub>3</sub>), 1.89 (t, *J* = 7.7 Hz, 24H, CH<sub>2</sub>CH<sub>3</sub>), –3.76 (dd, *J* = 14.7 Hz, *J* = 11.9 Hz, 1H, RhCH(CH<sub>3</sub>)CH<sub>2</sub>CO<sub>2</sub>H), –4.55 (dd, *J* = 14.7 Hz, *J* = 3.0 Hz, 1H, RhCH(CH<sub>3</sub>)CH<sub>2</sub>CO<sub>2</sub>H), –4.78 to –4.68 (m, 1H, RhCH(CH<sub>3</sub>)CH<sub>2</sub>CO<sub>2</sub>H), –4.94 (d, *J* = 6.1 Hz, 3H, RhCH(CH<sub>3</sub>)CH<sub>2</sub>CO<sub>2</sub>H). <sup>13</sup>C NMR (125 MHz, CDCl<sub>3</sub>): δ 170.03 (s, COOH), 141.83 (s, pyrrole α), 140.39 (s, pyrrole β), 99.25 (s, meso), 37.48 (s, α-C to carboxy), 19.76 (s, CH<sub>2</sub>CH<sub>3</sub>), 18.45 (s, CH<sub>2</sub>CH<sub>3</sub>), 18.18 (s, CH<sub>3</sub>), 17.11 (d, *J*<sub>C–Rh</sub> = 31.2 Hz, β-C to carboxy). IR (KBr): 2963, 2930, 2869, 1699, 1274, 1020 cm<sup>-1</sup>. UV-vis (benzene): λ<sub>max</sub> (log ε) 386.6 (1.23), 510.4 (0.12), 542.7 (0.37). FAB MS (*m*-nitrobenzyl alcohol matrix): *m/z*

(26) Whitlock, H. W.; Hanauer, R. *J. Org. Chem.* 1968, 33, 2169.  
 (27) Setsune, J.; Yoshida, Z.; Ogoshi, H. *J. Chem. Soc., Perkin Trans. I* 1982, 983.

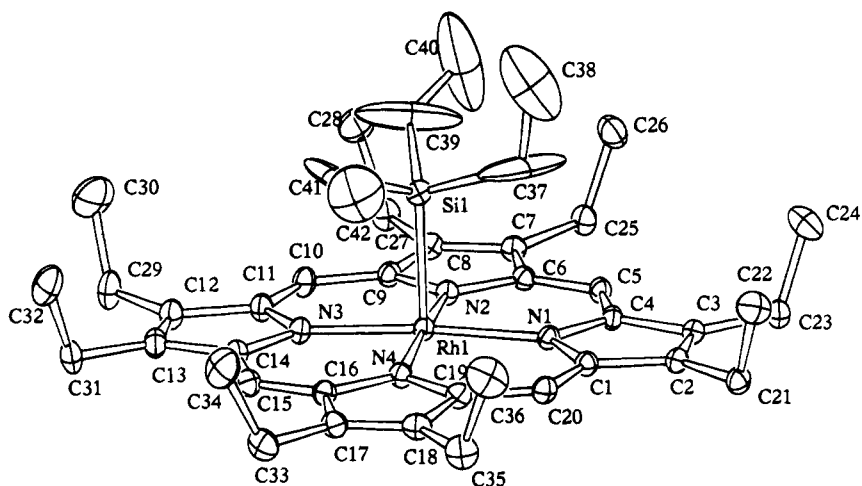


**Figure 1.** ORTEP drawing of  $\text{Rh}^{\text{III}}(\text{SiEt}_3)\text{OEP}$  showing thermal ellipsoids at the 30% probability level.

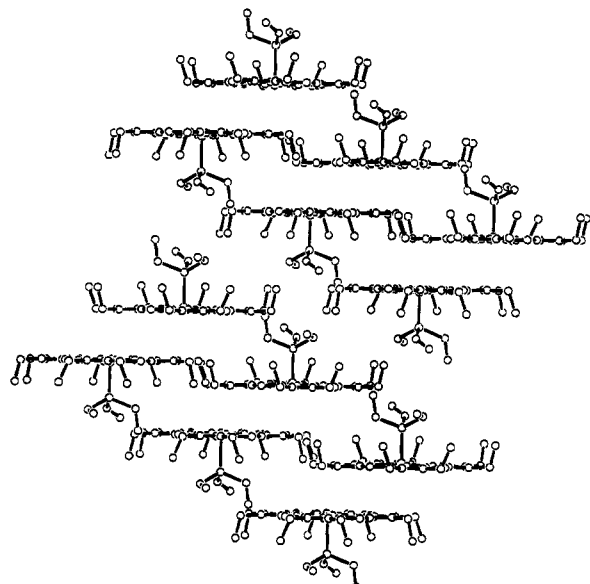


**Figure 2.** Crystal packing of  $\text{Rh}^{\text{III}}(\text{SiEt}_3)\text{OEP}$  in the direction of the  $b$  axis of the unit cell.

722 ( $\text{M}^+$ , 100). HRMS: calcd for  $\text{C}_{40}\text{H}_{51}\text{N}_4\text{O}_2\text{Rh}$  722.307, found 722.310.

**Reaction of  $[\text{Rh}^{\text{II}}\text{OEP}]_2$  with Triethylsilane (General Procedure).** To 53.4 mg of  $[\text{Rh}^{\text{II}}\text{OEP}]_2$  in dry degassed benzene (15 mL) was added triethylsilane (8; 0.66 mL, 4.1 mmol). The brown solution turned orange-red. The mixture was stirred at room temperature under Ar for 12 h. After the solvent was removed under reduced pressure, the residue was purified by column chromatography on silica gel (benzene:hexane = 1:2) to yield  $\text{Et}_3\text{SiRh}^{\text{III}}\text{OEP}$ ; yield 33.8 mg (54% based on  $[\text{Rh}^{\text{II}}\text{OEP}]_2$ ). The product was further purified by recrystallization from  $\text{CHCl}_3$ -hexane.

**Rh<sup>III</sup>(SiEt<sub>3</sub>)OEP (12).** Yield: 54%. TLC:  $R_f$  0.46 (SiO<sub>2</sub>, benzene:hexane = 1:5). <sup>1</sup>H NMR ( $\text{CDCl}_3$ , 500 MHz):  $\delta$  9.93 (s, 4H, meso), 3.99 (q,  $J$  = 7.6 Hz, 16H,  $\text{CH}_2\text{CH}_3$ ), 1.87 (t,  $J$  = 7.6 Hz, 24H,  $\text{CH}_2\text{CH}_3$ ), -1.59 (t,  $J$  = 8.0 Hz, 9H,  $\text{SiCH}_2\text{CH}_3$ ), -3.80 (q,  $J$  = 7.9 Hz, 6H,  $\text{SiCH}_2\text{CH}_3$ ). <sup>13</sup>C NMR (125 MHz,  $\text{C}_6\text{D}_6$ ):  $\delta$  141.63 (s, pyrrole  $\alpha$ -C), 141.32 (s, pyrrole  $\beta$ -C), 100.06 (s, porphyrin meso), 20.27 (s,  $\text{CH}_2\text{CH}_3$ ), 18.71 (s,  $\text{CH}_2\text{CH}_3$ ), 5.52 (s,  $\text{SiCH}_2\text{CH}_3$ ), 2.83 (s,  $\text{SiCH}_2\text{CH}_3$ ). <sup>29</sup>Si NMR ( $\text{CDCl}_3$ , 100 MHz):  $\delta$  51.98 (d,  $J_{\text{Si}-\text{Rh}} = 29.3$  Hz). IR (KBr): 2962, 2928, 2867, 1449, 1377, 1273, 1017, 994, 956, 845, 693  $\text{cm}^{-1}$ . UV-vis (benzene):  $\lambda_{\text{max}}$  (log  $\epsilon$ ) 393.4 (1.30), 509.6 (0.091), 542.2 (0.353). FAB MS (*m*-nitrobenzyl alcohol matrix):  $m/z$  750 ( $\text{M}^+$ , 100). HRMS: calcd for  $\text{C}_{42}\text{H}_{59}\text{N}_4\text{SiRh}$  750.356, found 750.360.

**Rh<sup>III</sup>(SiPh<sub>3</sub>)OEP (13).** Yield: 65%. TLC:  $R_f$  0.30 (SiO<sub>2</sub>, benzene:hexane = 1:3). <sup>1</sup>H NMR ( $\text{CDCl}_3$ , 500 MHz):  $\delta$  9.73 (s, 4H, meso), 6.69 (tt,  $J$  = 7.3 Hz,  $J$  = 1.2 Hz, 3H, 4'-H of Ph), 6.34 (dd,  $J$  = 7.3 Hz,  $J$  = 7.9 Hz, 6H, 3'-H of Ph), 4.13 (dd,  $J$  = 7.9 Hz,  $J$  = 1.2 Hz, 6H, 2'-H of Ph), 3.82–3.95 (m, 16H,  $\text{CH}_2\text{CH}_3$ ), 1.85 (t,  $J$  = 7.9 Hz, 24H,  $\text{CH}_2\text{CH}_3$ ). <sup>29</sup>Si NMR ( $\text{CDCl}_3$ , 100 MHz):  $\delta$  11.56 (d,  $J_{\text{Si}-\text{Rh}} = 35.7$  Hz). IR (KBr): 3075, 3045, 2961, 2928, 2867, 1448, 1274, 1059, 1021, 962, 698, 567  $\text{cm}^{-1}$ . UV-vis ( $\text{CHCl}_3$ ):  $\lambda_{\text{max}}$  (log  $\epsilon$ ) 544.2 (0.23), 508.8 (0.06), 393.3 (0.38), 380.5 (0.56). FAB MS (*m*-nitrobenzyl alcohol matrix):  $m/z$  894 ( $\text{M}^+$ , 100). HRMS: calcd for  $\text{C}_{54}\text{H}_{59}\text{N}_4\text{SiRh}$  894.356, found 894.360.

**Rh<sup>III</sup>(SiPhMe<sub>2</sub>)OEP (14).** Yield: 44%. TLC:  $R_f$  0.29 (SiO<sub>2</sub>, benzene:hexane = 1:5). <sup>1</sup>H NMR ( $\text{C}_6\text{D}_6$ , 500 MHz, chemical shift relative to  $\text{C}_6\text{H}_6$  7.20 ppm):  $\delta$  10.0 (s, 4H, meso), 6.71 (t,  $J$  = 7.3 Hz, 1H, 4'-H of Ph), 6.39 (dd,  $J$  = 7.3 Hz,  $J$  = 7.9 Hz, 2H, 3'-H of Ph), 4.21 (d,  $J$  = 8.0 Hz, 2H, 2'-H of Ph), 3.6–3.96 (m, 16H,  $\text{CH}_2\text{CH}_3$ ), 1.90 (t,  $J$  = 7.9 Hz, 24H,  $\text{CH}_2\text{CH}_3$ ), -3.61 (s, 6H,  $\text{SiCH}_3$ ). <sup>29</sup>Si NMR ( $\text{CDCl}_3$ , 100 MHz):  $\delta$  28.30 (d,  $J_{\text{Si}-\text{Rh}} = 30.2$  Hz). IR (KBr): 3046, 2961, 2927, 2866, 1458, 1379, 1273, 1233, 1018, 959, 808  $\text{cm}^{-1}$ . UV-vis (benzene):  $\lambda_{\text{max}}$  (log  $\epsilon$ ) 541.8 (0.42), 508.8 (0.11), 394.2 (1.34). FAB MS (*m*-nitrobenzyl alcohol matrix):  $m/z$  770 ( $\text{M}^+$ , 100). HRMS: calcd for  $\text{C}_{44}\text{H}_{55}\text{N}_4\text{SiRh}$  770.325, found 770.329.

**Rh<sup>III</sup>(SiOEtMe<sub>2</sub>)OEP (15).** Yield: 42%. TLC:  $R_f$  0.15 (SiO<sub>2</sub>, benzene:hexane = 1:2). <sup>1</sup>H NMR ( $\text{CDCl}_3$ , 500 MHz):  $\delta$  9.90 (s, 4H, meso), 3.90–3.98 (m, 16H,  $\text{CH}_2\text{CH}_3$ ), 1.81 (t,  $J$  = 7.7 Hz, 24H,  $\text{CH}_2\text{CH}_3$ ), -0.14 (q,  $J$  = 7.0 Hz, 2H,  $\text{SiOCH}_2\text{CH}_3$ ), -0.43 (t,  $J$  = 7.0 Hz, 3H,  $\text{SiOCH}_2\text{CH}_3$ ), -4.17 (s, 6H,  $\text{SiCH}_3$ ). <sup>29</sup>Si NMR ( $\text{CDCl}_3$ , 100 MHz):  $\delta$  37.24 (d,  $J_{\text{Si}-\text{Rh}} = 30.5$  Hz). IR (KBr): 2961, 2926, 2865, 1453, 1377, 1265, 1234, 1107, 1058, 1018, 957, 845, 811  $\text{cm}^{-1}$ . UV-vis ( $\text{CHCl}_3$ ):  $\lambda_{\text{max}}$  (log  $\epsilon$ ) 541.4 (0.25), 509.3 (0.07), 391.0 (1.06). FAB MS (*m*-nitrobenzyl alcohol matrix):  $m/z$  738 ( $\text{M}^+$ , 100). HRMS: calcd for  $\text{C}_{40}\text{H}_{55}\text{N}_4\text{OSiRh}$  738.320, found 738.313.

**Rh<sup>III</sup>(SnBu<sub>3</sub>)OEP (18).** To a solution of  $[\text{Rh}^{\text{II}}\text{OEP}]_2$  (26.4 mg, 121  $\mu\text{mol}$ ) in degassed benzene (6 mL) was added tributyltin hydride (0.12 mL, 446  $\mu\text{mol}$ ) under Ar. After the mixture was stirred for 21 h at room temperature, the benzene was distilled off and the residue was purified by a short column of silica gel (benzene:hexane = 1:2) to give **18** (18.8 mg, 49%). TLC:  $R_f$  0.60 (SiO<sub>2</sub>, benzene:hexane = 1:3). <sup>1</sup>H NMR ( $\text{C}_6\text{D}_6$ , 500 MHz, chemical shift relative to  $\text{C}_6\text{H}_6$  7.20 ppm):  $\delta$  10.07 (s, 4H, meso), 3.94 (q,  $J$  = 7.7 Hz, 16H,  $\text{CH}_2\text{CH}_3$ ), 1.93 (t,  $J$  = 7.7 Hz, 24H,  $\text{CH}_2\text{CH}_3$ ), 0.48–0.52 (br s, 9H,  $\text{SnCH}_2\text{CH}_2\text{CH}_2\text{CH}_3$ ), -0.76 to -0.60 (m, 6H,  $\text{SnCH}_2\text{CH}_2\text{CH}_2\text{CH}_3$ ), -2.54 to -2.38 (m, 6H,  $\text{SnCH}_2\text{CH}_2\text{CH}_2\text{CH}_3$ ). <sup>13</sup>C NMR (125 MHz,  $\text{C}_6\text{D}_6$  chemical shifts relative to  $\text{C}_6\text{D}_6$  128 ppm):  $\delta$  141.63 (s, pyrrole  $\alpha$ -C), 141.56 (s, pyrrole  $\beta$ -C), 99.92 (s, porphyrin meso), 27.14 (s,  $\text{SnCH}_2\text{CH}_2\text{CH}_2\text{CH}_3$ ), 26.92 (s,  $\text{SnCH}_2\text{CH}_2\text{CH}_2\text{CH}_3$ ), 20.00 (s,  $\text{CH}_2\text{CH}_3$ ),

18.66 (s,  $\text{CH}_2\text{CH}_3$ ), 13.35 (s,  $\text{SnCH}_2\text{CH}_2\text{CH}_2\text{CH}_3$ ), 7.47 (s,  $\text{SnCH}_2\text{CH}_2\text{CH}_2\text{CH}_3$ ).  $^{119}\text{Sn}$  NMR ( $\text{CDCl}_3$ , 186 MHz):  $\delta$  118.32 (d,  $J_{\text{Sn}-\text{Rh}} = 314.2$  Hz). IR (KBr): 2959, 2926, 2866, 1448, 1375, 1272, 1144, 1110, 1058, 1019, 993, 958, 843  $\text{cm}^{-1}$ . UV-vis (benzene):  $\lambda_{\text{max}}$  ( $\log \epsilon$ ) 381.4 (0.86), 298.7 (0.48), 509.1 (0.083), 541.1 (0.28). FAB MS (*m*-nitrobenzyl alcohol matrix): *m/z* 925 ( $\text{M}^+$ , 100). HRMS: calcd for  $\text{C}_{48}\text{H}_{71}\text{N}_4\text{RhSn}$  926.376, found 926.378.

**Rh<sup>III</sup>(SnPh<sub>3</sub>)OEP (19).** Yield: 44%. TLC  $R_f$  0.57 ( $\text{SiO}_2$ , benzene:hexane = 1:2).  $^1\text{H}$  NMR ( $\text{C}_6\text{D}_6$ , 500 MHz, chemical shift relative to  $\text{C}_6\text{H}_6$  7.20 ppm):  $\delta$  9.94 (s, 4H, meso), 6.77 (tt,  $J = 7.3$  Hz, 1.2 Hz, 3H, 4'-H of Ph), 6.55 (dd,  $J = 7.3$  Hz, 7.4 Hz, 6H, 3'-H of Ph), 4.93 (dd,  $J = 7.4$  Hz, 1.2 Hz, 6H, 2'-H of Ph), 3.80–3.93 (m, 16H,  $\text{CH}_2\text{CH}_3$ ), 1.88 (t,  $J = 7.6$  Hz, 24H,  $\text{CH}_2\text{CH}_3$ ).  $^{119}\text{Sn}$  NMR ( $\text{CDCl}_3$ , 186 MHz):  $\delta$  -121.57 (d,  $J_{\text{Sn}-\text{Rh}} = 412.9$  Hz). IR (KBr): 3059, 3046, 2964, 2929, 2866, 1447, 1376, 1273, 1145, 1059, 1021, 996, 962, 845, 727, 698  $\text{cm}^{-1}$ . UV-vis (benzene):  $\lambda_{\text{max}}$  ( $\log \epsilon$ ) 386.6 (1.09), 510.2 (0.073), 543.4 (0.27). FAB MS (*m*-nitrobenzyl alcohol matrix): *m/z* 986 ( $\text{M}^+$ , 100). HRMS: calcd for  $\text{C}_{54}\text{H}_{59}\text{N}_4\text{RhSn}$  986.282, found 986.290.

**X-ray Structure Determination of Rh<sup>III</sup>(SiEt<sub>3</sub>)OEP.** Purple crystals of Rh<sup>III</sup>(SiEt<sub>3</sub>)OEP were obtained by recrystallization from  $\text{CHCl}_3$ –hexane. Details of the crystal data, data collection, and data refinement are listed in Table 4. The structure was solved by direct methods<sup>28</sup> and expanded using Fourier techniques.<sup>29</sup>

**Acknowledgment.** We thank Dr. T. Kondo of the Division of Energy and Hydrocarbon Chemistry and H. Takagi for help in the X-ray crystallographic study and T. Kobatake for the measurements of mass spectra. We thank Anthony English of the Massachusetts Institute of Technology for proofreading the manuscript. This work was supported by a Grant-in-Aid for Specially Promoted Research (No. 04101003) from the Ministry of Education, Science, and Culture of Japan.

**Supplementary Material Available:** Tables of all bond distances and angles, anisotropic thermal parameters, torsion or conformation angles, and least-squares planes for **12** (17 pages). Ordering information is given on any current mast-head page.

OM940427C

---

(28) Sheldrick, G. M. *SHELXS86*. In *Crystallographic Computing 3*; Sheldrick, G. M., Kruger, C., Goddard, R., Eds.; Oxford University Press: Oxford, U.K., 1985; pp 175–189.

(29) DIRIDIF92: Beurskens, P. T.; Admiraal, G.; Beurskens, G.; Bosman, W. P.; Garcia-Granda, S.; Gould, R. O.; Smits, J. M. M.; Smykalla, C. Technical Report of the Crystallography Laboratory; University of Nijmegen, Nijmegen, The Netherlands, 1992.